SETAC PRESS

Environmental Toxicology and Chemistry, Vol. 18, No. 8, pp. 1733–1741, 1999

Printed in the USA
0730-7268/99 $9.00 + .00

Add to
HHF, BRO.1.13
(replace MS)

CHEMICAL AND BIOLOGICAL AVAILABILITY OF SEDIMENT-SORBED HYDROPHOBIC ORGANIC CONTAMINANTS

ELIZABETH M. LAMOUREUX† and BRUCE J. BROWNAWELL*‡
†Quantitative Environmental Analysis, LLC., 305 West Grand Avenue, Montvale, New Jersey 07645, USA
‡Marine Sciences Research Center, State University of New York at Stony Brook, Stony Brook, New York 11794-5000, USA

(*Received* 14 *April* 1998; *Accepted* 13 *October* 1998)

Abstract—The ability to predict accumulation levels of sediment-sorbed hydrophobic organic contaminants (HOCs) by deposit-feeding organisms based on sediment concentrations is limited in part by an incomplete understanding of the chemistry that controls assimilation efficiency. This study was designed to test the hypothesis that desorption is an important process that controls the bioavailability of HOCs to deposit-feeding organisms; we planned to do so by conducting desorption and bioavailability experiments with field-contaminated sediments collected from New York Harbor, New York, USA. Three classes of organic contaminants, polychlorinated biphenyls (PCBs), polycyclic aromatic hydrocarbons (PAHs), and linear alkylbenzenes (LABs) were studied. In order to address the effects of contaminant aging, we compared the contaminant desorption rates from sediments collected from surface and at depth in an area of known high-sediment accumulation to retarded intraparticle model predictions. Measured desorption rates of the LABs and the most hydrophobic PCBs compare well with model predictions. However, the PAH and less hydrophobic PCB desorption rates range from one to four orders of magnitude slower than model predictions. We postulate that these compounds are present in a resistant sedimentary phase and may represent only a small fraction of what was originally sorbed. The fraction of PCBs, PAHs, and LABs desorbed after 48 h correlate well with measured biota–sediment factors (BSFs) in *Yoldia limatula* that were exposed to the same sediments, indicating that desorption rate-limited assimilation. Several studies have related field BSFs with log K_{ow} and have observed a maximum at intermediate K_{ow}s (~6.0–6.5). This maximum may be due to predictably slow desorption of high-K_{ow} compounds and may be lower than predicted rates and extent of desorption of the low-K_{ow} compounds because of association with resistant phases.

Keywords—Desorption Bioavailability Polychlorinated biphenyls Polycyclic aromatic hydrocarbons Linear alkylbenzenes

INTRODUCTION

Accumulation of hydrophobic organic contaminants (HOCs) by benthic organisms can occur either from the aqueous phase or dietary exposure. As HOC partitioning to sediment increases with increasing octanol–water partition coefficient (K_{ow}), the importance of aqueous (pore water or overlying water) exposure pathways decreases relative to sediment ingestion. Sediment ingestion has been shown to be a significant or primary route of uptake to several species of deposit-feeding organisms exposed to HOC with log K_{ow} values ≥5.5 [1,2]. An equilibrium partitioning model, which predicts bioaccumulation levels that are independent of the route of uptake, has been proposed for the protection of benthic organisms [3]. However, field and laboratory studies have shown that organism body burdens sometimes depart significantly from equilibrium conditions. For example, accumulation of polycyclic aromatic hydrocarbons (PAHs) have been reported at levels lower than predicted by equilibrium partitioning calculations [4]. Conversely, accumulation of polychlorinated biphenyl (PCB) congener mixtures by deposit feeders are often higher than equilibrium partitioning predictions [5].

Kinetic bioaccumulation models typically consider organism ingestion, growth, chemical uptake from water, chemical elimination, chemical transformation within the organism, and assimilation of contaminant from the diet [6]. Under conditions in which sediment ingestion is the dominant exposure pathway, contaminant assimilation efficiency is one of the largest sources of uncertainty when modeling body burdens of contaminants. Contaminant assimilation efficiencies determined through short-term laboratory exposures for deposit-feeding invertebrates are relatively high. For example, hexachlorobiphenyl assimilation efficiencies of 16.1 to 46.4% have been reported for oligochaetes [2]; fluoranthene assimilation efficiencies of 56 and 22.4 to 46.0% have been measured for *Capitella* sp. I [7] and for *hydrobia* [8], respectively. However, assimilation of sediment organic matter (SOM) by deposit feeders is limited; typically only 5 to 30% of the total is in a bioavailable form [9]. Assuming that HOCs are uniformly distributed throughout the organic-matter pool, high contaminant and low SOM assimilation efficiencies implicate the rate and/or extent of desorptive release of contaminant from sediment during gut passage as a potential limiting mechanism. Assessment of the extent of desorption in the guts of deposit-feeding organisms is problematic. For some species, desorptive release into clean seawater may approximate the gut environment. For other species, desorptive release is likely enhanced by the presence of surfactants [10]. Weston and Mayer [11] have shown that absorption of PAH solubilized by the gut fluids of the polychaete *Arenicola brasiliensis* is nearly 100%, which highlights the importance of desorption extent on contaminant assimilation efficiencies. Although it is largely untested, it is possible that the processes that affect the relative

* To whom correspondence should be addressed (bbrownawell@ccmail.sunysb.edu).

Presented at the 218th Meeting of the American Chemical Society, Las Vegas, NV, USA, September 7–11, 1997.

desorption of various contaminants from sediments into clean seawater also limit HOC desorption when sediments are exposed to gut fluids.

Hydrophobic organic contaminant sediment desorption studies have demonstrated that an increase in HOC hydrophobicity generally leads to a decrease in the rate of sorption. Furthermore, the rate of desorption often decreases during the progression of a desorption experiment [12,13]. The fraction of chemical that desorbs at a slower rate is often said to reside in a resistant phase. In short-term laboratory experiments, this resistant phase has been modeled by considering a combination of intraaggregate diffusion and heterogeneity of sediment aggregate size [14]. Other experimental data, collected under conditions in which HOC has aged for long periods in the laboratory or field, show very slow desorption that cannot be easily described by intraaggregate pore-diffusion models [15,16]. It has been argued that such slow desorption might be the result of slow diffusion through more crystalline glassy organic geopolymer phases [16–19]. However, Holmén and Gschwend [20] point out that there is a strong inverse dependence of diffusivity on hydrophobicity in glassy-type polymers. Hence, an assumption of glassy-type organic matter resulted in a range of PAH diffusivities that was too large to explain the sorption variation of PAH observed in their study. Another potential explanation for limited desorption is association of the organic contaminant with soot or coal matrices. Gustafsson and coworkers [21] were able to account for higher-than-predicted partition coefficients of PAHs observed in Boston Harbor [22] and Mystic Lake, Massachusetts, USA, by quantifying the fraction of soot in these sediments and thereby calculating a soot-phase partition coefficient. Regardless of the mechanism, it is clear that under some environmental conditions, a fraction of sediment-associated contaminants becomes more resistant to desorption.

The objective of this study has been to compare the rate and extent of desorption of HOC into seawater with the extent to which these contaminants are accumulated by a deposit-feeding bivalve. Three HOC classes, which differ in structure and likely in matrix associations, were measured—PCBs, linear alkylbenzenes (LABs), and PAHs. Desorption and bioaccumulation experiments were conducted on surficial and deeper sediments collected from a single site in New York Harbor, New York, USA, in order to assess any effects of sediment depth on chemical and biological availability. Desorption experiments determined the maximum rate of desorption into seawater by use of a polymer resin with excess sorbent capacity [16]. Bioavailability experiments were conducted by incubating the subsurface deposit-feeding bivalve *Yoldia limatula* with sediments from the different core sections. We also discuss slow desorption as a potential mechanism that may limit the bioavailability of certain HOCs.

EXPERIMENTAL APPROACH

Sediment collection

Sediments were collected in May 1995 from a site located near Governors Island in New York Harbor at a water depth of 11.6 m. The site is in a high sediment-deposition area, with sediment-accumulation rates on the order of several centimeters per year [23]. Subsurface maxima in the concentrations of a variety of contaminants have been measured at this and other high-deposition sites in New York Harbor, which reflects a drop in contaminant inputs over the past couple of decades [24]. Two Soutar-type box cores (0.6 m^2), which were deployed from the research vessel *Onrust,* were sectioned into three intervals: 0 to 4 cm, 5 to 9 cm, and 10 to 14 cm, and identical intervals were combined and homogenized. Because of the high sediment accumulation, these sediments intervals reflect historical deposition of less than 10 year's time at the site. However, it would be difficult to assess the length of time during which contaminants may have been associated with sediment particles because of the dynamic cycling of sediments between bedded deposits and overlying waters in high-energy environments such as the Hudson Estuary/New York Harbor system. After collecting samples for HOC analysis, the remainder of the sediment sections were sieved on site with a 500-μm mesh screen and a minimal amount of seawater in order to remove detritus and biota. Sieved sediments were placed in acid-washed Nalgene® bottles (Nalgene, Rochester, NY, USA) and stored at 4°C for 1 month until the initiation of the bioavailability and desorption experiments. All sediments to be used in the desorption and bioavailability experiments were further sieved in the lab with a 63-μm mesh screen, using no more than a 2:1 ratio of seawater to sediment.

Desorption experiments

Desorption experiments were conducted utilizing the method of Carroll and coworkers [16]. XAD-4 Resin (Aldrich, Milwaukee, WI, USA) was prepared by first rinsing with deionized water and then refluxing successively with methanol, acetone/hexane (50/50), and methanol in a Soxhlet-like apparatus for 24 h. The resin was then rinsed with deionized water, placed in a clean jar (which was filled with deionized water), and refrigerated until use to prevent dehydration. Approximately 7 g wet (1.5–2 g dry) sediment, 10 ml of seawater, and approximately 2 g wet XAD-4 resin were placed in solvent rinsed 25-ml vials. The vials were placed in a rotating shaker (150 rpm) and maintained at 25°C. Vials were removed at 2, 5, 12, 48, 158, and 480 h after initiation of the experiment, and 0.5 g of potassium carbonate was added to enhance phase separation. The XAD-4 and sediments were separated by low-speed centrifugation, and both phases were frozen until analysis.

Bioavailability experiments

Three 10-L aquarium tanks, one for each of the three sediment intervals, were filled with seawater, and five 473-ml jars, each containing approximately 300 g of wet sediment (5-cm deep), were placed in the tanks. Exposures were conducted at room temperature (21°C), and the salinity of the water was 30‰. Three preweighed *Y. limitula,* purchased from the Woods Hole Marine Biological Laboratory (Woods Hole, Massachusettes, USA), were placed in each jar. Within 1 h, puffs of suspended sediment were visible, indicating the *Yoldia* were actively feeding. The tanks were aerated, and pH and salinity were monitored. The seawater in the tanks was replaced weekly. At each time point, organisms from one of the jars were removed, placed in clean sediment, and allowed to depurate for 24 h. Approximately 6 g of wet sediment was added to the remaining jars to replenish the sediment displaced by *Yoldia* feeding activity. The clams were then weighed, shucked, placed in preweighed centrifuge tubes, homogenized with a VirTis (Gardiner, NY, USA) tissue homogenizer, and frozen until extraction.

Analytical procedures

The extraction of PCBs, PAHs, and LABs from sediment, tissue, and XAD-4 resin samples followed a modification of

the method described in Lamoureux [25]. Wet sediment and tissue samples were placed in centrifuge tubes, and recovery standards were added for each compound class: 1-C9 alkylbenzene (AB), 1-C12AB, 1-C14AB (n-CmAB:n refers to the position of the alkyl chain to which the benzene ring is attached, and m refers to the chain length), PCBs 29 and 143, and *p*-terphenyl. Sediments and tissues were extracted sequentially with acetone, acetone:hexane (1:1), and hexane:dichloromethane (1:1), using a Cole Parmer 4710 Series, 600-W ultrasonic probe (Cole Parmer, Niles, IL, USA). After each extraction, samples were centrifuged, and supernatants were decanted and combined. XAD-4 Resin was extracted in a Soxhlet apparatus by refluxing with acetone:hexane (1:1) for 24 h. The organic solvent fraction of each sample was back-extracted with water, separated into a hexane phase, and concentrated. Sediment and XAD-4 samples were concentrated to approximately 1 ml, whereas organism samples were reduced to approximately 6 ml, and two 200-µl portions of the sample extract were removed for lipid weight analysis on a Cahn microbalance. The remaining tissue extract was reduced to 1 ml under a stream of nitrogen. The sample matrix was cleaned with a 1-cm i.d. column containing 7 g of silica gel (5% deactivated with water).

Polychlorinated biphenyls were analyzed on a Hewlett Packard 5890 gas chromatograph (GC; Hewlett Packard, Avondale, PA, USA) equipped with a 30-m DB-5 capillary column (J&W Scientific, Folsom, CA, USA) and an electron capture detector. The LABs and PAHs were analyzed on a Hewlett Packard 5890 GC equipped with a Hewlett Packard 5970A mass selective detector and a 30-m DB-5 capillary column (J&W Scientific). Linear alkylbenzene samples and standards were monitored in the selective ion mode for mass-to-charge ratios 91 and 105. Polycyclic aromatic hydrocarbon samples and standards were monitored in the selective ion mode for the following mass-to-charge ratios: 128, 142, 152, 156, 166, 170, 178, 190, 192, 202, 206, 228, 230, 252, and 276.

Polychlorinated biphenyl standards were prepared by combining Aroclors 1232, 1248, and 1262 (25:18:18) with the recovery standards PCB 29 and 143 in order to obtain response factors. Polychlorinated biphenyls in samples were quantified relative to PCB 29 and were corrected for recovery. Recovery of PCB 29 averaged 87.2 ± 14.8%, and recovery of PCB 143 averaged 101.2 ± 18.8%. Procedural blanks were subtracted from all samples and were generally less than 10% of sample PCB concentrations.

The LAB reference standard was prepared by combining a commercial mixture of all secondary isomers with linear alkyl chain lengths of 10, 11, 12, 13, and 14 (courtesy of R. Eganhouse), 26 isomers total, along with four 1-phenylalkanes (1-C9AB, 1-C10AB, 1-C12AB, and 1-C14AB). The masses of each component were estimated for the standard based on GC/flame ionization detector response of 1-phenyldecane. Individual LAB peaks in samples were calculated by comparing their response to that of 1-C10AB, which was added as an internal standard prior to injection and which was corrected for recovery. Mean recoveries were 83.0 ± 12.4% for 1-C9AB, 91.7 ± 14.3% for 1-C12AB and 92.6 ± 20.2% for 1-C14AB. Total LAB concentrations were obtained by summing the individual alkylbenzene concentrations and subtracting blank values, which fell below 10% of sample concentrations.

Individual PAH concentrations were determined by comparing their peak area response to that of *p*-terphenyl. Total PAH concentrations include the following PAHs: naphthalene; 1- and 2-methylnaphthalenes; 2,6-dimethylnaphthalene; acenaphthylene; acenapthene; 2,3,5-trimethylnaphthalene; fluorene; phenanthrene; anthracene; 1-, 2-, 3-, and 9-methylphenanthrenes; 3,6-dimethylphenanthrenes; fluoranthene; pyrene; benz(*a*)anthracene; chrysene; benzofluoranthenes; benz(*e*)pyrene; benz(*a*)pyrene; perylene; indeno(1,2,3-cd)pyrene; dibenzanthracene, and benzo(*ghi*)perylene. Identification was made by comparing peak retention times to those in standards injected on the same day. The recovery of *p*-terphenyl was 77.8 ± 17.9%. Procedural blanks, subtracted from all samples, were well below 10% of all sample PAH concentrations.

Total organic carbon was measured on a Carlo Erba EA1108 CHN Analyzer (CE Institute, Milan, Italy). Measurements were made relative to a sulphanilamide standard after removal of inorganic carbon with dilute hydrochloric acid. Disaggregated grain-size analysis was measured on a SediGraph® (MicroMetrics, Londonderry, NH, USA) in a sodium metaphosphate solution after prior removal of organic carbon with hydrogen peroxide [26], whereas aggregated grain size was determined through pipette analysis [27] without organic carbon removal.

Calculation of predicted and measured desorption rates

The rates and extent of desorption measured in these experiments were compared to predictions of the Wu and Gschwend radial intraparticle diffusion model [14]. The advantage of this mechanistic-based model is that it provides a priori predictions of desorption based on measurable sediment and HOC properties. It describes sorption as a reversible process, which includes aqueous-phase diffusion of HOC through the pores of aggregated particles, that is retarded by rapid partitioning between intraparticle fluid and organic matter. The numerical solution to this model can simulate the multicompartment sorption kinetic behavior first well described by Karickhoff [12]. The model has come under scrutiny in recent years because it cannot describe the very slow sorption observed in some experiments and because it ignores possible slow diffusion of HOC through natural organic matter [13]. We have compared our data to this model to both test the application of the model to marine sediments across a wide range of HOC and to determine under which conditions there are gross departures from the predictions of this simple model. For example, measured desorption rates much lower than those predicted by the model would be consistent either with very strong sorption (e.g., adsorption to soot carbon) or with incorporation into resistant phases (e.g., low-permeability geopolymers or protection by small pores or mineral coatings).

The radial diffusion coefficient employs a sorption rate constant (k), which is estimated from an average radius (r) of the particle aggregates and the effective diffusivity (D_{eff}).

$$k = \alpha \frac{D_{eff}}{r^2}$$

In this equation, α is a constant and D_{eff} is the effective (sorption-impeded) intraparticle diffusion coefficient (cm²/s) [14]. In this study, we have used the relationship from Karickhoff et al. [28] to estimate the sediment–water distribution coefficient (K_d) that is used in the calculation of D_{eff} from the fraction organic carbon of the sediment (f_{oc}) and the K_{ow} of the sorbate: $\log K_d = \log f_{oc} + \log K_{ow} - 0.21$. The K_{ow} values for PCBs [29], PAHs [30], and LABs [31] were taken from the literature. An average particle diameter of 20 µm, used in the D_{eff} cal-

Table 1. Total PCB, PAH, LAB, and TOC concentrations and grain size of Hudson River sediments

Depth interval (cm)	Total PCB (ng/g)	Total PAH (ng/g)	mp:p[a]	Total LAB (ng/g)	I:E[b]	Total organic carbon (%)	Median grain size (μm)[c]
0–4	415.9	5,887	0.7	1,282	1.8	3.62	3.91 (30.2)
5–9	450.1	5,638	1.2	1,854	1.7	3.72	3.60 (31.6)
10–14	494.7	6,135	0.9	1,777	1.6	3.31	3.74 (29.4)

[a] mp:p Ratio is defined as the ratio of 1-, 2-, 3-, and 9-methylphenanthrenes to phenanthrene.
[b] I:E Ratio is the ratio of 6- and 5-alkylbenzenes to 2-, 3-, and 4-alkylbenzenes.
[c] Indicates the median aggregated grain diameter.

culation, corresponds to a value intermediate between the mean aggregated and disaggregated diameters measured for each sediment (see Table 1).

The numerical solution to the Wu and Gschwend model provides desorption kinetic results that depart distinctly from first-order kinetic behavior, even when only a single particle radius is used. Much of the desorption kinetic data that we provide below also seem to show desorption behavior where the rate constant decreases over time. On the other hand, the desorption kinetics that we observed could be reasonably well described by a first-order model (r^2 = 0.76–1.0) for the majority of HOCs that we examined. The small number of time points (six) in our study precludes sophisticated kinetic treatments or robust comparisons between kinetic models. Therefore, in order to compare our results to Wu and Gschwend model predictions, three exercises were performed. For HOC desorption results that could be reasonably described by first-order desorption kinetic behavior (ln C_s vs time, where C_s is the sorbed HOC concentration), we compared observed first-order rate-constant measurements to first-order rate-constant estimates calibrated to the numerical solution of the Wu and Gschwend model when 50% of HOC has desorbed (when $t \sim 0.03\ r^2/D_{eff}$, or when $\alpha = 22.7$ for the condition when there is a diminishingly low fraction of chemical sorbed at equilibrium) [14]. For many of the lower molecular weight PCBs, the plots of ln C_s versus time could not be approximated by a first-order model and instead were fit to a two-compartment model [12], using JMP version 3.1.6.2 (SAS Institute, Cary, NC, USA). The parameters k_{fast}, k_{slow}, and the f_{fast} were determined, where f_{fast} ($f_{slow} = 1 - f_{fast}$) is the fraction of the sorbed HOC in a pool desorbing with rate constant k_{fast}. In most cases in which a two-compartment model was clearly needed to describe the data, the k_{fast} was slower than that predicted by the Wu and Gschwend model; thus, k_{slow} departed from the intraparticle diffusion model by an even greater extent. As so few data determined the three adjustable parameters in the two-compartment model, we place little statistical confidence on the values of k (especially k_{slow}). However, the values of k_{fast} do provide better-than–order of magnitude estimates of initial desorption to compare to intraparticle diffusion model predictions. A stricter comparison of our data to the numerical solution of the Wu and Gschwend model was conducted by comparing the extent of desorption measured at a given time to model prediction with the use of graphical solutions provided in Wu and Gschwend [14].

RESULTS

Sediment characterization

Total concentrations for each compound class increased slightly with depth (Table 1). The organic carbon content of the sediment decreased slightly with depth, whereas the median diameter of both aggregated and disaggregated measurements of the <63-μm fractions remained more constant over the sampling interval.

In addition to total PAH concentrations, methylphenanthrene to phenanthrene ratios (mp:p) ratios are reported on Table 1. This ratio, defined as the ratio of the sum of 1-, 2-, 3-, and 9-methylphenanthrene to phenanthrene, offers a means of estimating the relative abundance of PAHs derived from petrogenic (oil) and pyrogenic (combustion) sources, as PAHs that derive from petrogenic sources are known to contain a greater abundance of alkylated homologues than those that derive from pyrogenic sources [32]. An mp to p ratio of 0.5 to 1 is indicative of combustion-derived sources of PAH [32], whereas ratios of 3.14 and 2.36 have been measured in New York City sewage sludge [33], which reflects the significant amount of petroleum-derived inputs. As shown, the low mp to p ratio values measured in these New York Harbor sediments suggest that pyrogenic sources dominate the PAH signature that is preserved.

The relative distribution of internal (phenyl substitution position toward the middle of the chain) to external (phenyl substitution position toward the end of the chain) LAB isomers has been identified as a measure of the degree of degradation of the LAB mixture after it has entered the environment [34]. Values of greater than 1 for this internal to external ratio (I:E), defined as the ratio of 5- and 6-C12AB to 4-, 3-, and 2-C12AB, indicate some degree of degradation relative to commercial surfactant mixtures [34]. Internal to external ratio values reported in Table 1 are greater than 1, which indicates that some degree of degradation has occurred. The similarity of the I to E ratios calculated for the 0 to 4- and 10 to 14-cm sediment intervals suggests that little degradation has occurred after incorporation into the sediment bed. Our primary purpose in measuring this ratio in the sediments, however, was to use it as a baseline value for our experiments. Increases or decreases in this ratio can be used to investigate the effect of structure on isomer-specific desorption, bioavailability, and metabolism within an LAB homologue group.

HOC Desorption

The rate and extent of desorption of all compound classes was similar for all three depth intervals, indicating that the effect of the sediment aging following deposition and burial had not significantly hindered desorption of the contaminants in the deeper sediments (Fig. 1). Polychlorinated biphenyls showed the least impedance to desorption, with 20 to 40% remaining in the sediment after 480 h. The total PAH desorption rate and extent was less than that of the total PCBs, with 30 to 60% remaining in the sediments at the end of the ex-

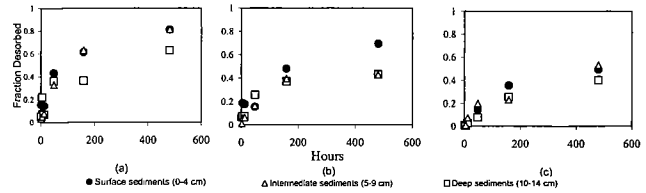

Fig. 1. The fraction of total polychlorinated biphenyls (**a**), polycyclic aromatic hydrocarbons (**b**), and linear alkylbenzenes (**c**) desorbed from New York Harbor surface (0–4-cm), intermediate (5–9-cm), and deep (10–14-cm) sediments over time.

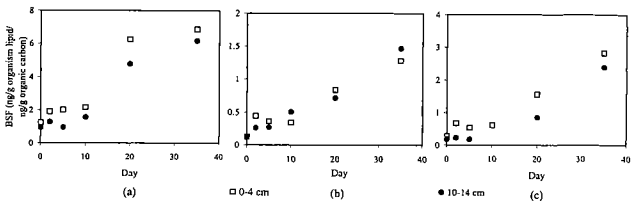

Fig. 3. Total polychlorinated biphenyl (**a**), polycyclic aromatic hydrocarbon (**b**), and linear alkylbenzene (**c**) compound biota–sediment factors for *Yoldia limatula* from surface (0–4-cm) and deeper (10–14-cm) sediments.

periments. Total LAB desorption was the most limited, with 55 to 60% of the initial concentration remaining in the sediment.

While total compound-class desorption patterns are useful for comparison, more can be learned from looking at the desorption rate of individual compounds. The desorption of PCB congeners 52, 101, 138, and 180 over time are shown on Figure 2a as examples of the relative desorption of a tetra-, penta-, hexa-, and heptachlorobiphenyls. Interestingly, the least hydrophobic congener, 52 (log K_{ow} = 5.84), had the most desorption-resistant fraction and appeared to exhibit the fastest shift from a fast to a slow desorption rate. The desorption rates of the most hydrophobic congeners, 138 and 180 (log K_{ow} = 6.83 and 7.36, respectively), appeared to be initially slower than the other two congeners and did not show a pronounced shift, which indicates that the desorption-resistant fraction of these congeners is small or that the time course of desorption was not followed long enough. Note that 88 and 86% of congeners 138 and 180, respectively, desorbed after 20 d. The low–molecular weight congeners fit well to a two-compartment model, however, as shown on Figure 2c.

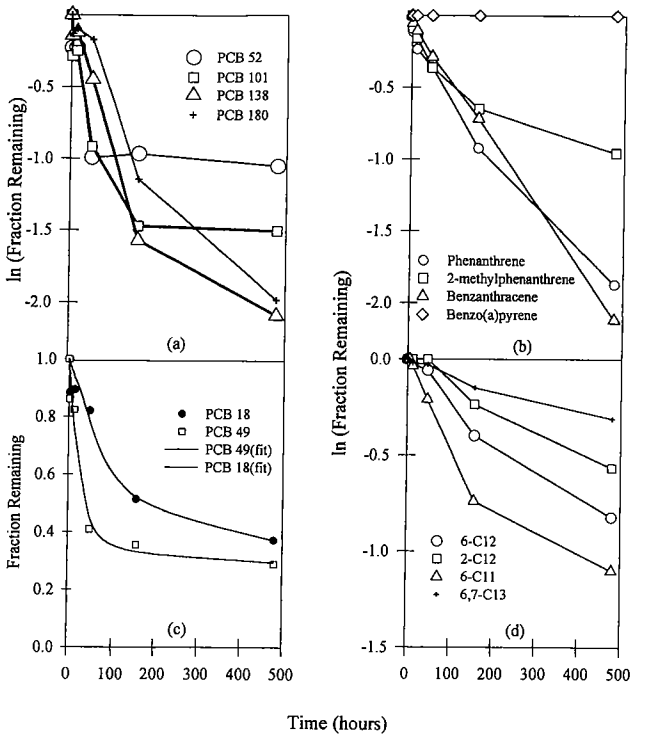

Fig. 2. The natural log of the fraction of individual (**a**) polychlorinated biphenyl (**b**) polycyclic aromatic hydrocarbon, and (**d**) linear alkylbenzene compounds remaining over desorption experiment time and (**c**) the fraction of two representative low–molecular weight PCB compounds remaining over time and fit to the two-box model. Rate information for these selected hydrophobic organic contaminants is provided in Table 2.

Differences in individual PAH compound desorption kinetics do not appear to be a simple function of K_{ow} (Fig. 2b). Benz[*a*]anthracene (log K_{ow} = 5.91) and phenanthrene (log K_{ow} = 4.57) desorbed at similar rates, whereas the overall desorption rate of 2-methylphenanthrene was slower (log K_{ow} = 5.01). Benzo[*a*]pyrene (log K_{ow} = 6.50) did not desorb over the time course of the experiment, despite having a K_{ow} value that was lower than PCB congener 138.

The desorption kinetics of the LAB compounds, plotted on Figure 2d, were much slower (note the change of scale) and more predictable in terms of hydrophobicity than were the desorption kinetics of the representative PCB and PAH compounds; LAB desorption rates increased with increasing chain length and hydrophobicity. The estimated K_{ow} values of LAB for a given chain length increased with increasing distance of the phenyl substitution position from the center of the chain [31]. The desorption patterns of these LAB compounds were consistent with their K_{ow} values in that the external (most hydrophobic) compounds desorbed more slowly than did the internal (less hydrophobic) LABs.

Bioaccumulation

The total compound class biota–sediment factors (BSFs) (ng/g organism lipid/ng/g sediment organic carbon) observed in *Y. limitula* over time are plotted on Figure 3. Significant PCB levels were measured in *Yoldia* prior to initiation of the experiment, as indicated by the y-intercept value. The lipid content of *Yoldia* declined over the time course of the experiment (percent lipid [wet weight] = 0.48–0.012*t*, *t* = days); however, the mean lipid contents at the beginning and the end of the experiment were not statistically different ($p > 0.05$). Little difference in bioaccumulation rate and extent was seen between the sediment intervals. Polychlorinated biphenyl, the compound class for which desorption was the greatest, also attained the highest levels of bioaccumulation in *Yoldia*. Although LABs exhibited the slowest desorption kinetics, they appeared to accumulate to a greater extent in *Yoldia* than the PAHs.

DISCUSSION

Comparison of measured and predicted desorption kinetics

The desorption patterns of the individual PCB, PAH, and LAB compounds plotted on Figure 2 are typical for each compound class in that the PAHs, LABs, and highest molecular-weight PCBs exhibit nearly first-order desorption kinetics, whereas the majority of the PCBs conform to a two-compartment model, with initially fast and then slow desorbing components. For comparison with the retarded/radial-diffusion

Table 2. Measured (surface-sediment) and predicted desorption rate constant examples

Compound[a]	log K_{ow}	$k_{first\ order}$	r^2	k_{fast} (10^{-3}/h)	k_{slow} (10^{-3}/h)	$k_{predicted}$ (10^{-3}/h)
PCB 18	5.24	—	—	8.4 (±0.12)	0.13 (±0.07)	646.0
PCB 49	5.85	—	—	37.4 (±0.52)	0.35 (±0.001)	151.0
PCB 52	5.84	—	—	44.0 (±0.97)	0.09 (±0.108)	155.0
PCB 101	6.38	—	—	32.3 (±0.58)	0.12 (±0.002)	42.7
PCB 138	6.83	8.3 (±1.5)	0.91	—	—	14.5
PCB 180	7.36	2.4 (±1.3)	0.94	—	—	2.0
Phenanthrene	4.57	3.5 (±0.2)	0.92	—	—	6,610.0
2-Methylphenanthrene	5.10	1.7 (±0.3)	0.99	—	—	1,550.0
Benzanthracene	5.91	4.3 (±0.4)	0.89	—	—	245.0
6-C11	7.45	2.4 (±0.4)	0.89	—	—	5.2
6-C12	8.01	1.8 (±0.2)	0.97	—	—	1.4
2-C12	8.19	1.2 (±0.09)	0.98	—	—	0.9
6,7-C13	8.56	0.7 (±0.05)	0.97	—	—	0.4

[a] PCB 18 = 2,2′,5′-trichlorobiphenyl; PCB 49 = 2,2′,4,5′-tetrachlorobiphenyl; PCB 52 = 2,2′,5,5′-tetrachlorobiphenyl; PCB 101 = 2,2′4,5,5′-pentachlorobiphenyl; PCB 138 = 2,2′,3,4,4′,5′-hexachlorobiphenyl; PCB 180 = 2,2′,3,4,4′,5,5′-heptachlorobiphenyl.

model predictions, desorption rate constants (k) for the PAH, LAB, and the high–molecular weight PCB compounds were calculated from a first-order kinetic model that approximates the observed desorption behavior (desorption rate constants and correlation coefficients are given on Table 2). The desorption kinetics of the remainder of the PCBs were fit to a two-box model in order to obtain desorption rate constants for a labile pool (k_{fast}) and a more resistant pool (k_{slow}). For this comparison, k_{fast} was used for PCBs with log K_{ow} values less than 6.7. Measured log k values were plotted against the log k values predicted from the retarded/radial-diffusion model on Figure 4a, and relevant kinetic parameters for select HOCs are given in Table 2. Measured and predicted rate constants were in close agreement in both magnitude and dependence on K_{ow} for the LABs and approximately one-half of the PCBs. The PCBs that showed close agreement were the most hydrophobic PCBs, with log K_{ow} values that were greater than 6.2. The PCBs for which measured k values fell below predicted values were congeners that possessed log K_{ow} values that were less than 6.2. Note that for the lower K_{ow} PCBs, k_{slow} departs from $k_{predicted}$ by an even greater amount than Figure 4a indicates (for examples, see Fig. 2). The measured PAH rate constants were far below model predictions.

The k_{slow} calculated from this study of field-contaminated sediments (sorption time scales of years to decades) for congener 49, a tetrachlorobiphenyl (2,2′,4,5′-CB), was 3.5×10^{-4}/h (Table 2), which is slower than available literature k_{slow} values measured for tetrachlorobiphenyls derived from studies using laboratory-spiked sediments (sorption time scales of days to weeks); k_{slow} values were 1.72 to 2.54×10^{-3}/h for congener 65 (2,3,5,6-CB) [35] and 0.8 to 5×10^{-3}/h for congener 54 (2,2′,6,6′-CB) [36]. In contrast, the measured k_{slow} for congener 118, a pentachlorobiphenyl (2,3′,4,4′,5-CB), 5.2×10^{-3}/h, was much more comparable to the k_{slow} value of 0.98 to 2.01×10^{-3}/h that was reported by Cornelissen and coworkers [35], which suggests that the rate of slow desorption decreases with increasing time of contaminant association with sediments for lower molecular-weight congeners but perhaps not for high–molecular weight congeners As can be seen in Figure 2c, few data constrain the estimate of k_{slow} that was derived from a two-compartment model. However, a comparison of our estimates to those measured in other long-term PCB-desorption experiments may suggest differences in the role of aging for low– and high–molecular weight PCB-congener desorption kinetics. Future experiments would need to be done to confirm our k_{slow} estimates.

Possible explanations for the deviation from desorption rate constants predicted by the Wu and Gschwend retarded intraparticle diffusion model for the less hydrophobic compounds and their observed biphasic desorption patterns include the following: (1) the existence of micropores within the sediment matrix that are available to the smaller compounds but that prohibit the penetration of larger compounds on the basis of size and shape; (2) two types of organic-matter phases within particle aggregates; "elastomer" and "glassy," in which HOC diffusion is relatively fast and slow, respectively [13,37]; and (3) strong partitioning to soot phases within the sediment. The close agreement of the most hydrophobic compounds with the retarded intraparticle diffusion model and the lack of agreement of the least hydrophobic compounds with the model is supported by the first explanation. In this scenario, the labile PCB pool could decrease over time, either during transport of contaminated sediment in the water column or following deposition, thereby leaving behind a slowly reequilibrating resistant pool. The smaller, less hydrophobic congeners, because they are more soluble, may have been removed from the labile pool more quickly, thereby leaving a greater fraction in the resistant phase.

The low–molecular weight PCB desorption behavior also may be explained by the intra–organic-matter diffusion model; the observed multiphasic desorption behavior could be due to desorption from both elastomer (fast) and condensed (slow) sedimentary organic-matter phases [13,17,18]. It is more difficult to explain the single-compartment desorption behavior of the more hydrophobic HOC compounds (Fig. 2) with an intra–organic-matter diffusion model, unless the higher molecular-weight compounds are excluded from sorption volumes within more condensed organic-matter phases or unless there has not been sufficient time (greater than years to decades) for the larger compounds to diffuse into this matrix.

In contrast to the less hydrophobic PCBs, the PAHs did not exhibit biphasic desorption patterns, which are indicative of multiple sorptive phases, despite the fact that the K_{ow} values of all the PAHs that had measurable desorption rates were less than $10^{5.91}$. Hence, it is likely that the sorption mechanisms leading to the slow desorption of the low–molecular weight

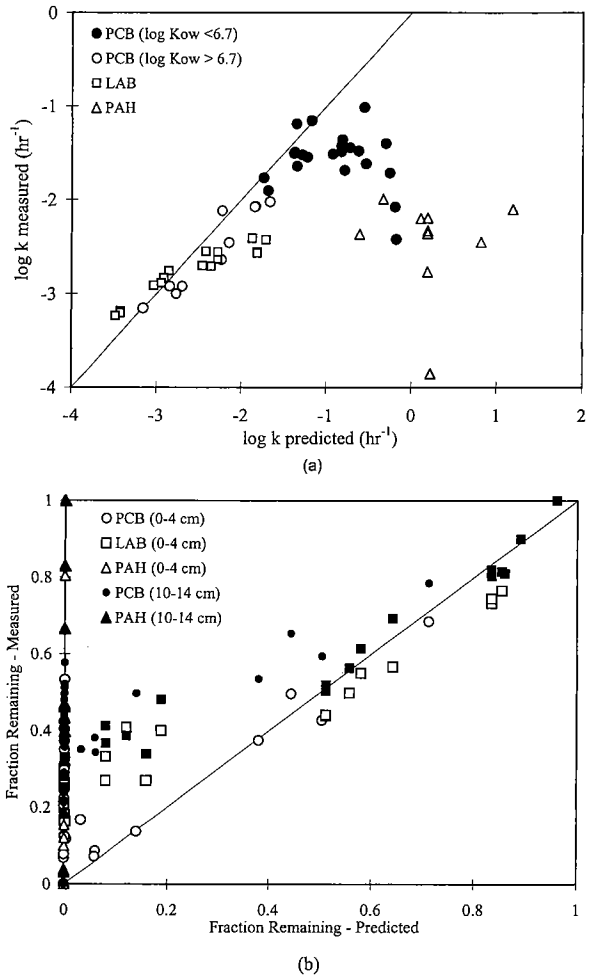

Fig. 4. (**a**) Measured desorption rate constants plotted against rate constants predicted from the first-order approximation of the Wu and Gschwend retarded intraparticle diffusion model and (**b**) the measured fraction of individual compounds remaining on sediments at 20 d plotted against the fraction predicted to be remaining from the numerical solution of the retarded intraparticle diffusion model [14].

PCBs differ from those controlling the PAH sorption. As mentioned, the PAH composition in these sediments denotes a combustion source. Additionally, the apparent partition coefficients of the PAHs, calculated from the measured effective diffusion coefficients in the Wu and Gschwend model, are much higher than predicted from organic-matter partitioning models. The resulting log K_d for phenanthrene, for example, is 6.1; three orders of magnitude higher than the K_d value of 2.7 predicted for New York Harbor sediment with 3.6% organic matter. Previous investigators have attributed high apparent PAH K_ds to the presence of soot [21,22]. It is likely that a significant fraction of the PAHs present in these sediments is associated with soot, but it is also possible that planar PAHs are able to penetrate intraaggregate pores more easily than the other compound classes studied.

The measurable fraction of individual compounds remaining on 0 to 4- and 10 to 14-cm sediments after 20 d of desorption were compared to those predicted to be remaining from the numerical solution of the retarded intraparticle diffusion model [14] on Figure 4b. The compounds that showed reasonable agreement were the most hydrophobic (log K_{ow} $\geq$6.2). The majority of the compounds, however, were predicted to be 100% desorbed on this time scale because of their

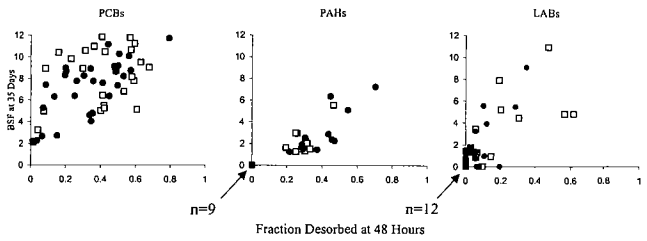

Fig. 5. Individual polychlorinated biphenyl, polycyclic aromatic hydrocarbon, and linear alkylbenzene compound biota–sediment factors at 35 d plotted against the fraction desorbed at 48 h for 0–4 (open squares)-and 4–10 (closed circles)-cm sediments.

relatively small hydrophobicity, but large fractions of these compounds were still associated with the sediments. Note that there was little difference between the results for the 0 to 4- and 10 to 14-cm depth intervals.

Relationship between bioaccumulation and desorption

A clear relationship exists between the *Yoldia* BSFs measured at day 35 of the bioaccumulation experiment and the fraction of the compound desorbed in 48 h (Fig. 5), especially for the PAHs and LABs. The 48-h desorption time point was used for this comparison as an upper limit on the gut residence time of *Yoldia* (G. Lopez, unpublished data). The presence of a number of compounds that neither desorbed nor were bioaccumulated and the strength of the correlation between BSFs and the fraction desorbed ($r^2 > 0.78$ for PAHs and LABs) was consistent with the hypothesis that desorption is an important control on bioaccumulation. Variability in the relationship between BSFs and the fraction desorbed for PCBs may have been due, in part, to the relatively high initial PCB levels in *Yoldia*.

An interesting illustration of the coupling of desorption and bioaccumulation is provided by examining the LAB internal to external ratio over time in both experiments (Fig. 6). The internal to external ratio peaked during the desorption experiment at 48 h because of the initially slower desorption rate of the external isomers. The internal to external ratio in *Yoldia* continued to increase until it reached a final value of 10, while the ratio remained fairly constant in the sediments in both experiments. Similarly, high internal to external ratios were measured in two species of echinoids collected from the 106

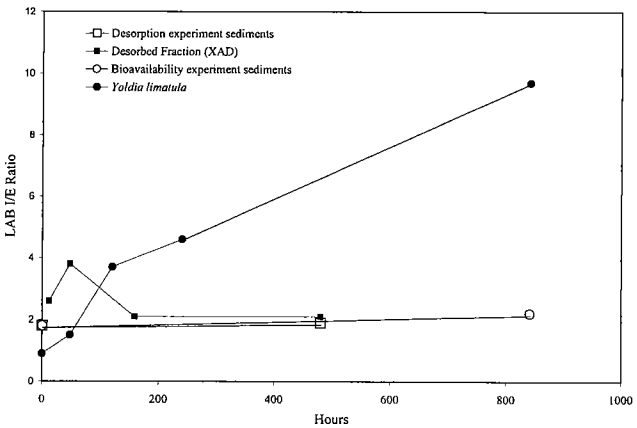

Fig. 6. The linear alkylbenzene internal to external ratio (ratio of 6-C12 and 5-C12 to 4-C12, 3-C12, and 2-C12) over time in bioavailability-and desorption-experiment sediments, the desorbed fraction, and *Yoldia limatula*.

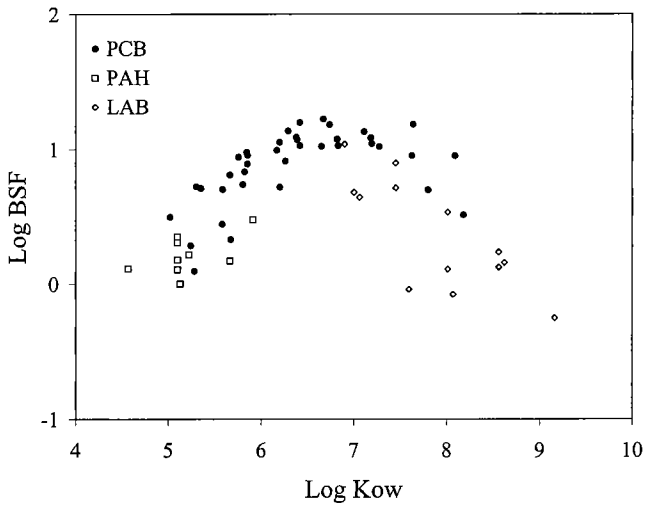

Fig. 7. Log biota–sediment factors of individual polychlorinated biphenyl, polycyclic aromatic hydrocarbon, and linear alkylbenzene compounds in *Yoldia limatula* plotted against log K_{ow}.

Mile Sewage Sludge Dump site, while sediment internal to external ratios remained low [25]. The external LAB isomers have been shown to be metabolized faster than the internal isomers [34]. Slower desorption of the external isomers, within a gut transit-time window, coupled with preferential metabolism of these isomers could also contribute to the high internal to external ratio observed in *Yoldia* in this study (and previously, for echinoids from the Sludge Dump site).

The relationship of log BSF with log K_{ow} for all compounds measured for surface sediments are shown on Figure 7. Note that the high levels of BSF (maximum values >10) probably reflect the loss of lipids by *Yoldia* during the experiment. Slow desorption of both low (<6) and high (>7.5) K_{ow} compounds may also provide an explanation for the parabolic relationship of BSF with K_{ow}, which has been observed in this study and elsewhere [38,39]. Previous investigators have suggested that depressed bioaccumulation of more soluble HOC is related to faster elimination rates for lower K_{ow} compounds [38,39]. We hypothesize that in some sedimentary regimes, the bioavailability of lower molecular-weight compounds may be limited by slow desorption from a resistant phase.

The mechanism responsible for the relationship between desorption extent at 48 h and accumulation of HOC by *Yoldia* (Fig. 6) is not clear. Additionally, it is unknown whether similar relationships might be observed for other species. Future work should compare the desorption of contaminants in systems that mimic species-specific environments with their accumulation by these organisms in order to determine the effect that these environments have on controlling desorption rate–limited assimilation.

The relationship between chemical and biological availability of sorbed HOC has long been recognized as a useful management tool (i.e., equilibrium partitioning). The establishment of this relationship becomes problematic, however, when considering the interplay between thermodynamic and kinetic limited processes on contaminant assimilation. This and other studies show that characteristic desorption times for HOCs from field-aged sediments into clean seawater can be long compared to gut residence times, consistent with possible desorption-rate limitation on assimilation. This scenario could also occur in the presence of surfactants if the gut residence time of sediment is not of sufficient length to enable equilibration of HOCs with gut fluid. Thus, desorption tests, whether into clean water, gut juice, or other model solution, will require additional comparisons with assimilation efficiencies before they can be used with confidence in the assessment of bioavailability.

CONCLUSIONS

The results of this study demonstrate that chemical availability is correlated with the biological availability of HOCs to *Y. limatula* and suggest that it is worth exploring further whether bioaccumulation might be predicted by short-term desorption studies. Further work should include additional species, sediment types, and desorption solutions. Desorption rates can be closely predicted from the Wu and Gschwend model for high–molecular weight compounds but not for low–molecular weight compounds and polycyclic aromatic compounds. This study also suggests that the lower biota–sediment accumulation factors for the low–molecular weight compounds may also be related to limited chemical availability of these compounds and not just to faster elimination into the aqueous phase. Future work should explore whether limited availability of PAHs and of lower chlorinated PCBs is due to a soot-phase association or to their ability to access micropore and/or polymer-limited sorption volumes.

Acknowledgement—This research was supported by a Tibor T. Polgar Fellowship awarded to E.M. Lamoureux by the Hudson River Foundation and by Hudson River Foundation grant 003-96-A. The authors thank the crew of the *Onrust* for sampling assistance and G. Cornelissen, P.C.M. van Noort, Th.E.M. ten Hulscher, A. McElroy, and two anonymous reviewers for their thoughtful comments on this manuscript.

REFERENCES

1. Fowler SW, Polikarpov GG, Elder DL, Parsi P, Villeneuve JP. 1978. Polychlorinated biphenyls: Accumulation from contaminated sediments and water by the polychaete *Nereis diversicolor*. *Mar Biol* 48:303–309.
2. Klump JV, Krezoski JR, Smith ME, Kaster JL. 1987. Dual tracer studies of the assimilation of an organic contaminant from sediments by deposit feeding oligochaetes. *Can J Fish Aquat Sci* 44:1574–1583.
3. Di Toro DM, et al. 1991. Technical basis for establishing sediment quality criteria for nonionic organic chemicals using equilibrium partitioning. *Environ Toxicol Chem* 10:1541–1583.
4. Paine MD, Chapman PM, Allard PJ, Murdoch MH, Minifie D. 1996. Limited bioavailability of sediment PAH near an aluminum smelter: Contamination does not equal effects. *Environ Toxicol Chem* 11:2003–2018.
5. Lake JL, Rubinstein NI, Lee H II, Lake CA, Heltshe J, Pavignano S. 1990. Equilibrium partitioning and bioaccumulation of sediment-associated contaminants by infaunal organisms. *Environ Toxicol Chem* 9:1095–1106.
6. Thomann RV, Connolly JP, Parkerton TF. 1992. An equilibrium model of organic chemical accumulation in aquatic food webs with sediment interaction. *Environ Toxicol Chem* 11:615–629.
7. Forbes VE, Forbes TL, Holmer MH. 1996. Inducible metabolism of fluoranthene by the opportunistic polychaete, *Capitella* sp. I. *Mar Ecol Prog Ser* 132:63–70.
8. Forbes EF, Forbes TL. 1997. Dietary absorption of sediment-bound fluoranthene by a deposit-feeding gastropod using the ^{14}C:^{51}Cr dual-labeling method. *Environ Toxicol Chem* 16:1002–1009.
9. Mayer LM. 1989. The nature and determination of non-living sedimentary organic matter as a food source for deposit feeders. In Lopez G, Taghon GL, Levington JS, eds, *Ecology of Deposit Feeders*. Springer-Verlag, New York, NY, USA, pp 98–113.
10. Mayer LM, et al. 1996. Bioavailability of sedimentary contaminants subject to deposit-feeder digestion. *Environ Sci Technol* 30:2641–2645.
11. Weston DP, Mayer LM. 1998. Comparison of in vitro digestive

fluid extraction and traditional in vivo approaches as measures of polycyclic aromatic hydrocarbon bioavailability from sediments. *Environ Toxicol Chem* 17:830–840.
12. Karickhoff SW. 1980. Sorption kinetics of hydrophobic pollutants in natural sediments. In Baker RA, ed, *Contaminants and Sediments,* Vol 2. Analysis, Chemistry and Biology. Ann Arbor Science, Ann Arbor, MI, USA, pp 193–205.
13. Pignatello JJ, Xing B. 1995. Mechanisms of slow sorption of organic chemicals to natural particles. *Environ Sci Technol* 30: 1–11.
14. Wu S, Gschwend PM. 1988. Numerical modeling of sorption kinetics of organic compounds to soil and sediment particles. *Water Resour Res* 24:1373–1383.
15. Pignatello JJ, Ferrandino FJ, Huang LQ. 1993. Elution of aged and freshly added herbicides from a soil. *Environ Sci Technol* 27:1563–1571.
16. Carroll KM, Harkness MR, Bracco AA, Balcarcel RR. 1994. Application of a permeant/polymer diffusional model to the desorption of polychlorinated biphenyls from Hudson River sediments. *Environ Sci Technol* 28:253–258.
17. Brusseau ML, Rao PSC. 1989. The influence of sorbate–organic matter interactions on sorption nonequilibrium. *Chemosphere* 18: 1691–1706.
18. Weber WJ, McGinley PM, Katz LE. 1992. A distributed reactivity model for sorption by soils and sediments. 1. Conceptual basis and equilibrium assessments. *Environ Sci Technol* 26:1955–1962.
19. Xing B, Pignatello JJ, Gigliotti B. 1996. Competitive sorption between atrazine and other organic compounds in soils and model sorbents. *Environ Sci Technol* 30:2432–2440.
20. Holmén BA, Gschwend PM. 1997. Estimating sorption rates of hydrophobic organic compounds in iron oxide- and aluminosilicate clay–coated aquifer sands. *Environ Sci Technol* 31:105–113.
21. Gustafsson Ö, Haghseta F, Chan C, MacFarlane J, Gschwend PM. 1997. Quantification of the dilute sedimentary soot phase: Implications for PAH speciation and bioavailability. *Environ Sci Technol* 31:203–209.
22. McGroddy SE, Farrington JW. 1995. Sediment porewater partitioning of polycyclic aromatic hydrocarbons in three cores from Boston Harbor, Massachusetts. *Environ Sci Technol* 29:1542–1550.
23. Olsen CR, Simpson HJ, Peng T-H, Bopp RF, Trier RM. 1981. Sediment mixing and accumulation rate effects on radionuclide depth profiles in Hudson Estuary Sediments. *J Geophys Res* 86: 11020–11028.
24. Bopp RF, Simpson HJ. 1989. Contamination of the Hudson River: The sediment record. In National Research Council, *Contaminated Marine Sediments—Assessment and Remediation.* National Academy Press, Washington, DC, USA, pp 401–416.
25. Lamoureux EM. 1995. The distribution of linear alkylbenzenes, polychlorinated biphenyls, and polynuclear aromatic hydrocarbons in sediments and biota at the 106-Mile Deep Water Disposal site. MS thesis. State University of New York at Stony Brook, Stony Brook, NY, USA.
26. Coakley JP, Syvitski JPM. 1991. Sedigraph technique. In Syvitski, JP, ed, *Principles, Methods, and Application of Particle Size Analysis.* Cambridge University Press, Cambridge, UK, pp 129–142.
27. Folk RL. 1968. *Petrology of Sedimentary Rocks.* Hemphill, Austin, TX, USA, pp 37–57.
28. Karickhoff SW, Brown DS, Scott TA. 1979. Sorption of hydrophobic pollutants on natural sediments. *Water Res* 13:241–248.
29. Hawker DW, Connell DW. 1988. Octanol–water partition coefficients of polychlorinated biphenyl congeners. *Environ Sci Technol* 22:382–387.
30. Schwarzenbach R, Gschwend PM, Imboden DM. 1993. *Environmental Organic Chemistry.* John Wiley & Sons, New York, NY, USA.
31. Sherblom PM, Gschwend PM, Eganhouse RP. 1990. Aqueous solubilities, vapor pressures, and 1-octanol–water partition coefficients for C9-C14 linear alkylbenzenes. *J. Chem Eng Data* 37:394–399.
32. Prahl FG, Crecellus E, Carpenter R. 1984. Polycyclic aromatic hydrocarbons in Washington coastal sediments: An evaluation of atmospheric and riverine routes of introduction. *Environ Sci Technol* 18:687–693.
33. Takada H, Farrington JW, Bothner MH, Johnson CG, Tripp BW. 1994. Transport of sludge-derived organic pollutants to deep-sea sediments at Deep Water Dump site 106. *Environ Sci Technol* 28:1062–1072.
34. Takada H, Ishiwatari R. 1990. Biodegradation experiments of linear alkylbenzenes (LABs): Isomeric composition of C12 LABs as an indicator of the degree of LAB degradation in the aquatic environment. *Environ Sci Technol* 24:86–91.
35. Cornelissen G, Van Noort PCM, Govers AJ. 1997. Desorption kinetics of chlorobenzenes, polycyclic aromatic hydrocarbons, and polychlorinated biphenyls: Sediment extraction with Tenax® and effects of contact time and solute hydrophobicity. *Environ Toxicol Chem* 16:1351–1357.
36. Coates JT, Elzerman AW. 1985. Desorption kinetics for selected PCB congeners from river sediments. *J Contam Hydrol* 1:191–210.
37. Young TM, Weber WJ. 1995. A distributed reactivity model for sorption by soils and sediments. 3. Effects of diagenetic processes on sorption energetics. *Environ Sci Technol* 29:92–97.
38. Oliver BG. 1984. Uptake of chlorinated organics from anthropogenically contaminated sediments by oligochaete worms. *Can J Fish Aquat Sci* 41:878–883.
39. Landrum PF. 1989. Bioavailability and toxicokinetics of polycyclic aromatic hydrocarbons sorbed to sediments for the amphipod *Pontoporeia hoyi. Environ Sci Technol* 23:588–595.